Effect of protonation on the photophysical properties of 4-substituted and 4,7-disubstituted quinazoline push-pull chromophores

Rodrigo Plaza-Pedroche, Dimitris Georgiou, Mihalis Fakis, Arnaud Fihey, Claudine Katan, Françoise Robin-Le Guen, Sylvain Achelle, Julian Rodríguez-López

Effect of protonation on the photophysical properties of 4-substituted and 4,7-disubstituted quinazoline push-pull chromophores.

Rodrigo Plaza-Pedroche,[a] Dimitris Georgiou,[b] Mihalis Fakis,[b,*] Arnaud Fihey,[c] Claudine Katan,[c] Françoise Robin-le Guen,[c] Sylvain Achelle,[c,*] Julian Rodríguez-López[a,*]

[a] Universidad de Castilla-La Mancha, Área de Química Orgánica, Facultad de Ciencias y Tecnologías Químicas, Avda. Camilo José Cela 10, 13071 Ciudad Real, Spain. E-mail: julian.rodriguez@uclm.es

[b] University of Patras, Department of Physics, GR-26504 Patras, Greece. E-mail: fakis@upatras.gr

[c] Univ Rennes, CNRS, ISCR (Institut des Sciences Chimiques de Rennes) - UMR 6226, F-35000 Rennes, France. E-mail: sylvain.achelle@univ-rennes1.fr

TOC

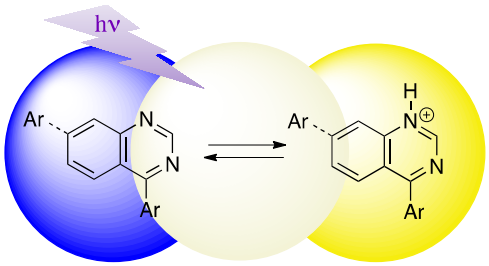

Abstract. White-light emission from single molecular systems has attracted a great deal of attention due to their advantages over multicomponent emitters. Azaheterocyclic push-pull derivatives have been demonstrated to be white emitters by combining neutral and protonated forms in the appropriate ratio, although limited cases of white-light emission have been reported from quinazoline derivatives. Herein, we describe a series of push-pull 4-substituted and 4,7-disubstituted quinazolines that show white photoluminescence both in solution and in the solid state. All of the materials were prepared by straightforward Suzuki–Miyaura cross-coupling reactions and the compounds exhibited remarkable emission solvatochromism. In some cases the presence of acid prompted the appearance of emission bands of complementary colors. Thus, multicolor photoluminescence, including white light, could be finely tuned by the controlled protonation of the electron-deficient quinazoline ring.

Keywords: fluorescence; push-pull chromophores; quinazolines; white-light emission.

1. Introduction

During the past decade there has been great interest in the design of push-pull azaheterocyclic chromophores due to their high tunability and the sensitivity of their photophysical properties to the environment.[1-5] In these structures, the nitrogen heterocycles are generally used as the electron-withdrawing part. These compounds exhibit intense positive emission solvatochromism, which is characteristic of compounds that undergo an intramolecular charge transfer (ICT) upon excitation.[6-9] These materials are also sensitive to the presence of acids,[10-15] metal cations,[16,17] and various biomolecules[18-20] due to the possibility of protonation, complexation, and the formation of hydrogen bonds with the nitrogen atom of the azaheterocycle, respectively. Push-pull nitrogen heterocyclic systems have also been designed for fluorescence sensing of nitroaromatic explosives.[21-23]

Although sensitivity to acids has been used primarily for sensing applications,[24-27] a more recent application concerns white light emission. The protonation of azaheterocyclic push-pull derivatives generally leads to emission quenching. Nevertheless, in certain cases, red-shifted emission is observed with an appropriate combination of nitrogen π-deficient heterocycles and electron-donating groups.[28-30] Thus, when neutral and protonated forms are combined, white light can be obtained both in solution and in solid state.[31-33] White organic light emitting diode (WOLED) devices have been fabricated by means of this strategy.[34,35]

Pyrimidinyl fragments have a stronger electron-withdrawing character than other diazinyl and pyridinyl groups due to the positions of the two nitrogen atoms. The electron-withdrawing strength can be enhanced by annelation to a phenyl ring to give a quinazoline.[1,36] Quinazoline is also a stronger base than pyrimidine (pK_a ~3.3 vs ~1.1).[37] The protonation of the first nitrogen atom affects the subsequent protonation of the second nitrogen atom, requiring a significantly lower pH. In fact, it has been reported that the protonation of the first nitrogen atom in pyrimidine leads to a second $pK_a \approx -6.3$.[28]

Quinazoline chromophores have only been studied in recent years and their push-pull derivatives have mainly been based on quinazolin-2-yl and quinazolin-4-yl fragments.[35,38-43] In particular, some of us have described a set of amino-substituted aryl-, styryl-, and arylethynylquinazolines.[44] It was found that all of these compounds exhibit emission quenching upon protonation.

In the work reported here, we designed a series of six 4-substituted and 4,7-disubstituted quinazoline push-pull chromophores with carbazolyl and methoxynaphthyl groups (Scheme 1). These substituents were selected because they revealed efficient white light emission upon controlled protonation.[31,32] To the best of our knowledge, these are the first examples of D-π-A-π-D chromophores with a 4,7-diarylquinazoline central core. The photophysical properties and white light emission were studied by steady-state and femtosecond to nanosecond time-resolved spectroscopy.

2. Results and discussion

2.1. Synthesis

Compounds **1** and **2** were obtained in moderate to good yields by Suzuki–Miyaura cross coupling of 4-chloroquinazoline and 7-bromo-4-chloroquinazoline, respectively, with the corresponding boronic acid (Scheme 1). It should be noted that the π-electron-deficient character of the quinazoline ring enabled the oxidative addition of palladium into the chloride-carbon bond with a classical ligand such as triphenylphosphine.[44-47]

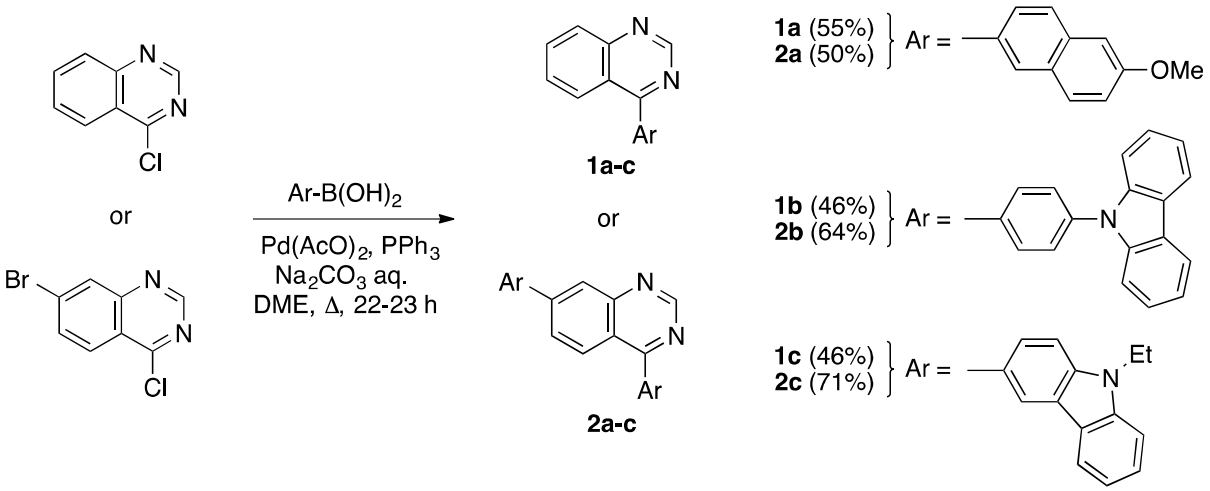

Scheme 1. Synthesis of compounds **1** and **2**.

2.2. Electronic structures of neutral and protonated compounds

In an effort to gain insights into the electronic structure of this series of molecules and the impact of the protonation, ground state DFT calculations were carried out on the neutral and the two possible protonated forms (see Scheme 2) of the compounds. The frontier orbitals of the neutral compounds **1a** and **2a** are depicted in Figure 1 (see Figures S1 and S2 of the Supporting Information for **1b**–**2b** and **1c**–**2c**, respectively). The π frontier orbitals are spatially well separated in the **1a**–**1c** subseries of mono-substituted molecules. The HOMO is located on the donor aryl substituent while the LUMO is on the quinazoline acceptor moiety. The nature of the donor group has a slight impact on the HOMO-LUMO energy gap, with respective values of 4.01 eV, 3.82 eV and 4.00 eV for **1a**, **1b** and **1c**.

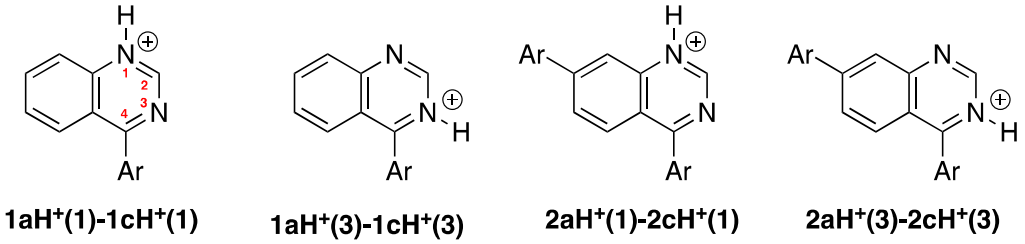

Scheme 2. Possible protonated forms of the compounds under study.

In the cases of **2a**–**2c**, where two identical substituents are attached, the HOMO is now split into HOMO and HOMO-1, which are located on either one or the other donor moiety (see Figure 1 for compound **2a**). The energy difference between the two occupied levels is non-negligible (see Table S1 in the Supporting Information), thus transcribing the non-symmetric character of the disubstituted compounds. Nevertheless, upon addition of a second substituent, the electronic structure of the compounds did not markedly change and the HOMO-LUMO energy gap is only slightly reduced: e.g., from 4.01 eV for **1a** to 3.96 eV for **2a** (all electronic gaps are given in Table S1 of the Supporting Information).

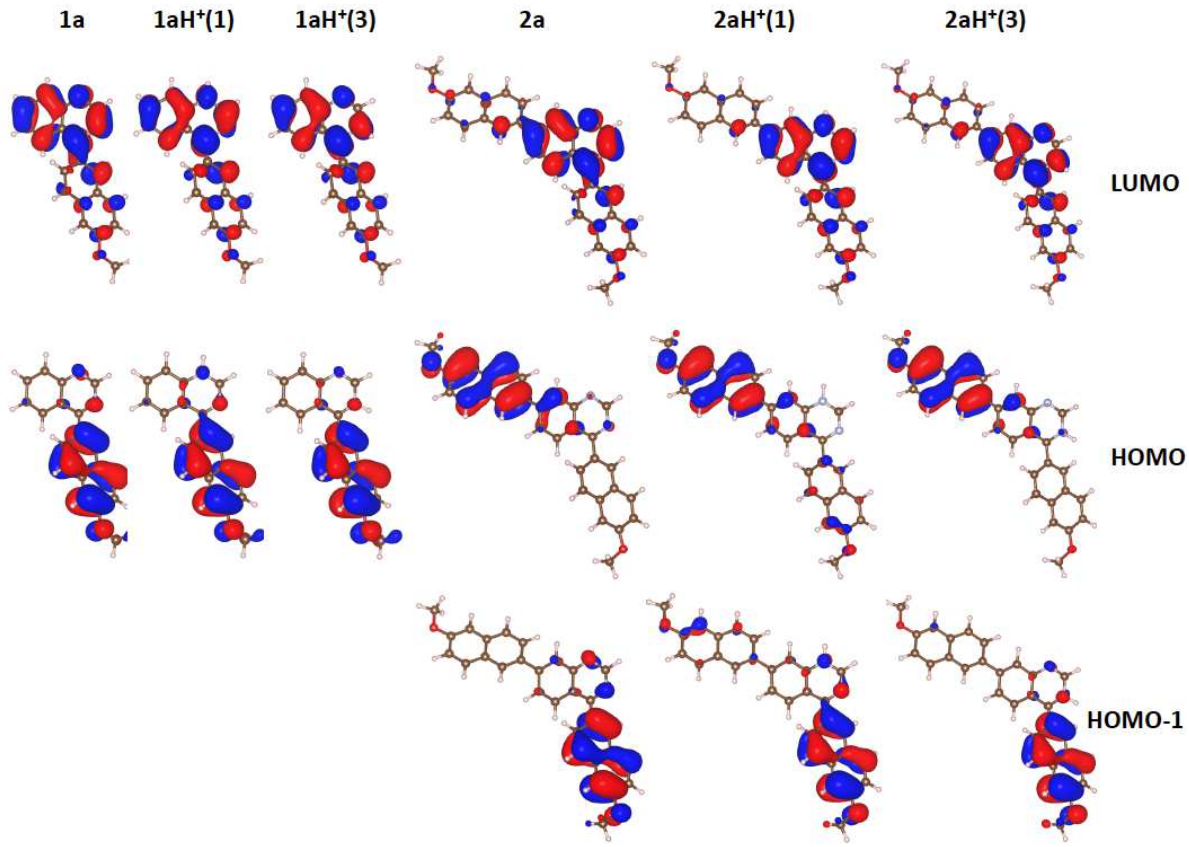

Figure 1. Frontier molecular orbitals (isovalue: 0.025) for neutral and protonated compounds **1a** and **2a** (PBE0/6-311+G(d,p), CH_2Cl_2).

Protonation of the quinazoline unit can be achieved on two different nitrogen atoms, as depicted in Scheme 2. The protonation of position 3 appears *a priori* less favorable due to

steric hindrance as the proton in this case is close to the aryl donor group, while such an effect is absent for protonation on position 1. This difference in steric hindrance does not consistently impact the computed ground-state structures. For instance, within the series of compounds the dihedral angle between the quinazoline and the aryl donor group varies in the range 35–45° without any clear trend in terms of the protonation site. The free energy differences between the two protonation sites for each compound are listed in Table 1. It appears that sites 1 and 3 are in most cases very close in energy, i.e., within 2 kcal mol^{-1}, although protonation on site 1 leads in all cases to the most stable isomer. Upon addition of a second substituent, the population ratio of site 3 increases up to 38% for **2b**. Such ratios are of course dependent on the computational level of theory and definitive quantitative predictions are difficult to make for such small energy differences. For the sake of comparison, the energy differences obtained with a range-separated hybrid functional are also provided in Table S2 of the Supporting Information. Although discrepancies in values are observed, similar trends arise and this indicates that site 1 is always preferred, while the population of site 3 remains non-negligible. These findings are consistent with a very recent report that the stabilities of two experimentally observed protonation isomers is indistinguishable based both on similar DFT and wave-function calculations.[48]

Table 1. Computed free energy differences in kcal mol^{-1} between the two protonated forms ($H^+(1)$/$H^+(3)$) of **1a**–**1c** and **2a**–**2c**, in CH_2Cl_2 (PBE0/6-311+G(d,p)). The energy of the most stable form is set to zero and the Boltzmann population is indicated in parenthesis.

Compd	$H^+(1)$	$H^+(3)$
1a	0.00 (74%)	0.61 (26%)
1b	0.00 (94%)	1.64 (6%)
1c	0.00 (81%)	0.86 (19%)
2a	0.00 (68%	0.44 (32%)
2b	0.00 (62%)	0.30 (38%)
2c	0.00 (70%)	0.51 (30%)

After protonation the change in the frontier molecular orbitals is insignificant and they present a similar topology (see Figure 1 for **1a** and **2a**), although both the HOMO and LUMO levels are stabilized. This stabilization is more pronounced for the LUMO orbital located on the quinazoline moiety on which the protonation takes place, thus resulting in a slight decrease of density on position 4 for H^+(1) and on positions 2 and 4 for H^+(3). This change is accompanied by a significant decrease in the electronic gap of roughly 1 eV. For instance, this value drops from 4.01 eV for **1a** to 3.02 eV for **1aH^+(1)** and 3.24 eV for **1aH^+(3)**. This decrease is similar for the disubstituted analogs, i.e., from 3.96 eV for **2a** to 2.92 eV for **2aH^+(1)** and 2.98 eV for **2aH^+(3)**. This difference between the electronic structures of neutral and protonated dyes is expected to yield distinguishable spectroscopic behavior.

2.3. Steady state spectroscopy in solution

The UV-vis and photoluminescence (PL) spectroscopic data for compounds **1** and **2**, recorded in CH_2Cl_2 at room temperature, are summarized in Table 2. As an example, the normalized spectra of compounds **1** are presented in Figure 2 (see Figure S3 in the Supporting Information for compounds **2**). All of the compounds absorbed light in the UV region and emitted light in the blue-green region. For the monosubstituted compounds **1**, the absorption maxima increased in the order λ_{abs}(**1a**) < λ_{abs}(**1b**) < λ_{abs}(**1c**). In terms of emission, the 4-(carbazol-9-yl)phenyl derivative **1b** was the most red-shifted and this led to a particularly high Stokes shift of 9205 cm^{-1}. The same trends were observed for the di-substituted quinazolines **2**. Chromophores **2** exhibited similar or slightly red-shifted absorption and emission maxima with respect to their monosubstituted analogs **1**, with a two-fold enhancement of the molar extinction coefficient. Regarding the fluorescence quantum yield, the disubstituted methoxynaphthyl quinazoline **2a** was significantly more emissive (Φ_F = 0.37) than the monosubstituted analog **1a** (Φ_F = 0.10). However, mono- and disubstituted carbazolyl derivatives **1b/2b** and **1c/2c** showed similar quantum yields (Φ_F = 0.65–0.77).

Table 2. UV-vis and photoluminescence (PL) data for compounds **1** and **2** in CH_2Cl_2 solution.

Compd[a]	λ_{abs} (nm)	ε ($mM^{-1}\,cm^{-1}$)	λ_{em} (nm)	Φ_F[b]	Stokes shift (cm^{-1})	τ (ns)	k_r ($10^9\,s^{-1}$)	k_{nr} ($10^9\,s^{-1}$)
1a	335	14.0	443	0.10	7277	6.47	0.015	0.14
1b	341	14.6	497	0.65	9205	7.26	0.089	0.048
1c	349, 361	15.4, 14.5	454	0.77	5674	3.93	0.19	0.058
2a	342	30.6	463	0.37	7641	3.14	0.12	0.20
2b	342	30.3	503	0.71	9359	6.95	0.10	0.041
2c	351, 370	30.6, 31.3	471	0.71	5796	3.38	0.21	0.086

[a] All spectra were recorded at room temperature at c = 1.5–3.0 × 10^{-5} M. [b] Fluorescence quantum yield (±10 %) determined relative to that of quinine sulfate in 0.1 M H_2SO_4 (Φ_F = 0.54).

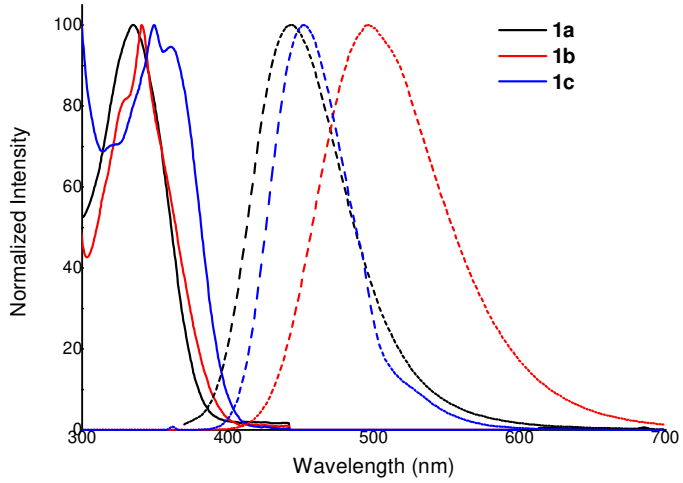

Figure 2. Normalized absorption (solid lines) and emission (dashed lines) spectra of compounds **1a** (black), **1b** (red), and **1c** (blue) in CH_2Cl_2 solution. Excitation performed at absorption maxima.

The results of the solvatochromic behavior in a series of aprotic solvents are summarized in Table 3. The PL spectra and the color changes observed upon UV irradiation for compound **2b** are shown in Figure 3 (see Figures S4–S8 in the Supporting Information for all compounds). As expected for push-pull derivatives, positive emission solvatochromism was observed in all cases. This phenomenon is due to the stabilization of a highly polar excited state in polar solvents.[49,50] Nevertheless, the emission solvatochromic range is

relatively limited, which is also a typical feature of chromophores with this kind of π-conjugated bridge and moderately strong electron-donating groups.[8,9]

Table 3. Emission solvatochromism of compounds **1** and **2** in various aprotic solvents.

Compd	Cyclohexane 30.9[a]	Toluene 33.9[a]	THF 37.4[a]	CH_2Cl_2 40.7[a]	Acetone 42.2[a]	MeCN 45.6[a]	DMSO 45.1[a]
1a	422	424	433	443	450	462	471
1b	420	437	473	497	517	541	548
1c	417	426	441	454	464	479	488
2a	393, 422	425	446	463	479	495	515
2b	408	442	482	503	529	560	563
2c	411	426	451	471	485	507	515

[a] $E_T(30)$ Dimroth–Reichardt polarity parameter in kcal mol^{-1}.[51]

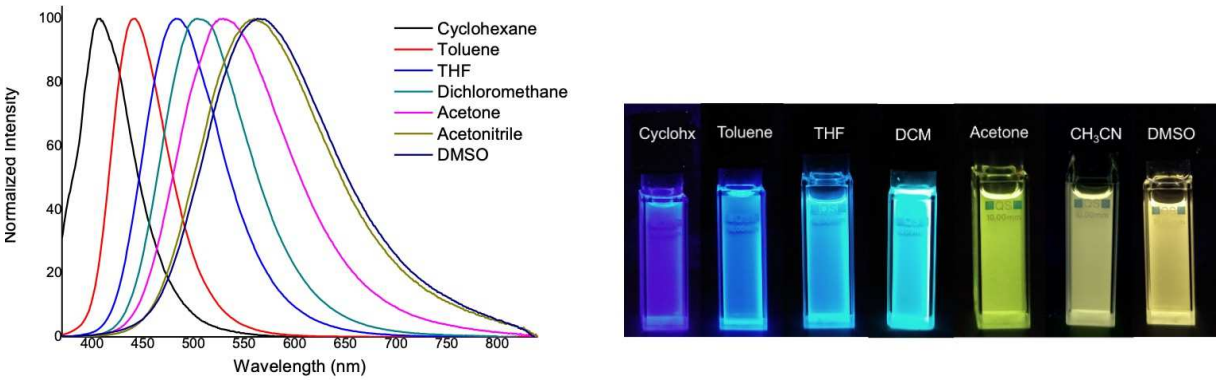

Figure 3. Normalized emission spectra and fluorescence color changes experienced by **2b** in different aprotic solvents. Pictures were taken in the dark upon irradiation with a hand-held UV lamp (λ_{exc} = 365 nm, 24 W).

The photophysical properties of compounds **1** and **2** were also studied in acidic conditions in a 10^{-2} M solution of camphorsulfonic acid (CSA) in CH_2Cl_2. The results are summarized in Table 4. The UV-vis and PL spectra of compounds **1** are shown in Figure 4 (see Figure S9 in the Supporting Information for compounds **2**). As one would expect, in all cases red-shifted absorption and emission spectra were observed with respect to neutral conditions. This observation is consistent with protonation of the quinazoline ring, which reinforces its electron-withdrawing ability and enhances the ICT. On the other hand, the

emission was partially or completely quenched in almost all cases except for compound **1a**, for which the fluorescence quantum yield increased upon protonation (from 0.10 to 0.26).

Table 4. UV-vis and photoluminescence (PL) data for compounds **1** and **2** in acid solution (10^{-2} M CSA in CH_2Cl_2).

Compd[a]	λ_{abs} (nm)	ε (mM^{-1} cm^{-1})	λ_{em} (nm)	Φ_F[b]	Stokes shift (cm^{-1})
1a	300, 415	8.6, 19.4	556	0.26	6111
1b	291, 323, 337, 442	31.2, 11.5, 11.6, 12.1	743	<0.01	9165
1c	267, 292, 341, 451	27.5, 23.8, 12.1, 25.9	614	0.04	5886
2a	273, 304, 428	46.8, 24.0, 37.0	630	0.09	7491
2b	292, 325, 338, 450	54.4, 33.9, 32.3, 22.5	758	<0.01	9030
2c	267, 295, 327, 469	28.9, 45.3, 22.9, 37.9	636	0.18	5599

[a] All spectra were recorded at room temperature at c = 1.5–3.0 × 10^{-5} M. [b] Fluorescence quantum yield (±10%) determined relative to fluorescein in 0.1 M NaOH (Φ_F = 0.79) as standard.

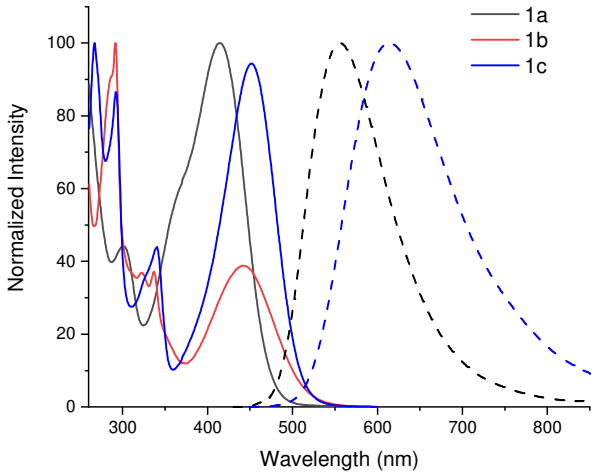

Figure 4. Normalized absorption (solid lines) and emission (dashed lines) spectra of compounds **1a** (black), **1b** (red), and **1c** (blue) in a 10^{-2} M solution of CSA (large excess) in CH_2Cl_2. Excitation performed at absorption maxima.

The addition of CSA to a CH_2Cl_2 solution of **1a** led to the progressive attenuation of the absorption band at 335 nm upon increasing the concentration of acid, whereas a new red-shifted band corresponding to the protonated species appeared at 415 nm. The spectra showed an isosbestic point at 359 nm and this is characteristic of an equilibrium between two species (Figure 5, left). Furthermore, a progressive color change from colorless to pale yellow was

observed with the naked eye (Figure 6a). In terms of emission, a new broad band at 556 nm gradually replaced that of the neutral species at 443 nm, with an isoemissive point at 490 nm (Figure 5, right). Under UV irradiation, the neutral solution of **1a** exhibited blue luminescence, whereas the solution of the protonated form of this compound showed a green-yellow emission. The controlled addition of three equivalents of CSA gave CIE coordinates (0.28, 0.33) close to those of pure white light (0.33, 0.33) under excitation at 360 nm (Figures 6b and 6c, Table 5). Similar behavior was observed for **1c**, **2a**, and **2c**. Thus, white emission could be observed when neutral and protonated forms of complementary colors were present in the appropriate ratio. In contrast, the protonation of **1b** and **2b** resulted in a progressive extinction of the emission (see Figures S11–S15 and S17–S21 in the Supporting Information for all compounds).

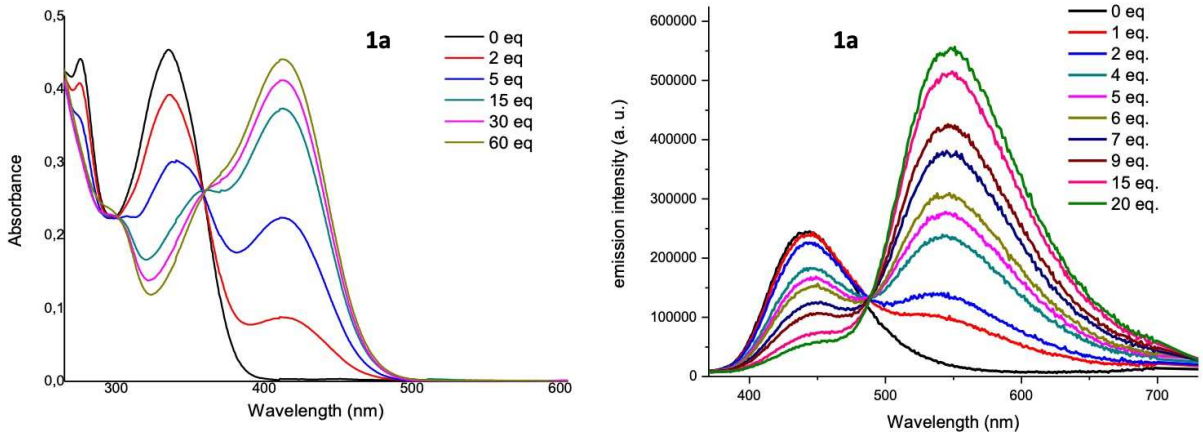

Figure 5. Changes in the absorption (left) and emission (right, λ_{exc} = 360 nm) spectra of a CH_2Cl_2 solution of **1a** upon addition of CSA.

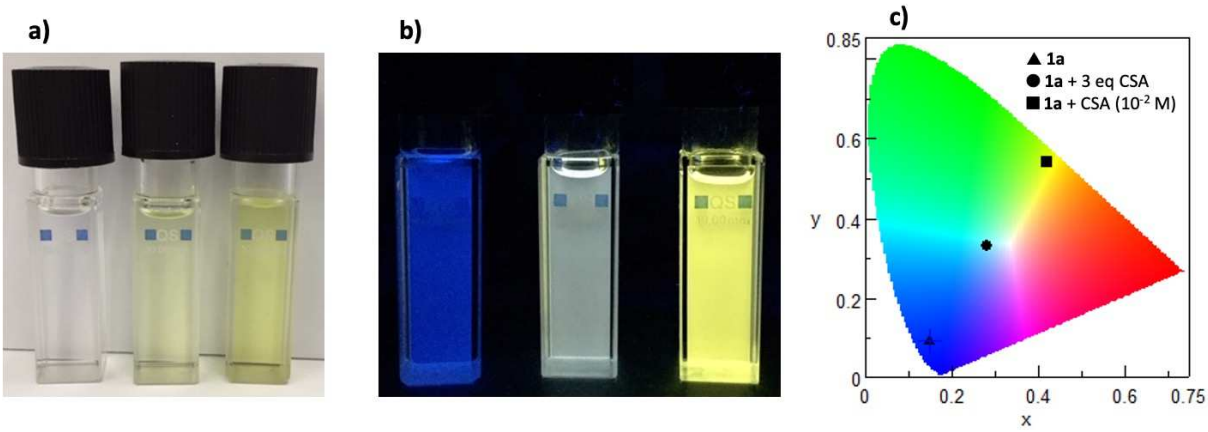

Figure 6. Changes in the color of a CH_2Cl_2 solution of **1a** ($c = 3.0 \times 10^{-5}$ M) after the addition of 3 (middle) and 100 equivalents of CSA (right): a) under visible light; b) under a hand-held UV lamp (365 nm, 24 W). c) Chromaticity of the fluorescence colors in a 1931 CIE diagram (λ_{exc} = 360 nm).

Table 5. CIE coordinates for compounds **1** and **2** in solution.

Compd	Chromaticity coordinates (x,y)		
	Neutral form[a]	Protonated form[b]	Mixture of neutral and protonated forms
1a	(0.15, 0.09)	(0.42, 0.54)	(0.28, 0.33)[c]
1b	(0.21, 0.38)	--	--
1c	(0.15, 0.10)	(0.53, 0.42)	(0.35, 0.31)[d]
2a	(0.16, 0.16)	(0.55, 0.43)	(0.34, 0.32)[e]
2b	(0.23, 0.43)	--	--
2c	(0.15, 0.19)	(0.58, 0.41)	(0.33, 0.31)[f]

[a] In CH_2Cl_2 solution. [b] In acid solution (10^{-2} M CSA in CH_2Cl_2). [c] 3 equivalents of CSA (λ_{exc} = 360 nm). [d] 16 equivalents of CSA (λ_{exc} = 390 nm). [e] 15 equivalents of CSA (λ_{exc} = 380 nm). [f] 5 equivalents of CSA (λ_{exc} = 400 nm).

In all of the compounds reported here, except for **1b** and **2b**, multicomponent fluorescence spectra with distinct but also overlapping contributions from the neutral and protonated species were clearly observed when CSA was added to the initial CH_2Cl_2 solutions. In addition to conventional steady-state fluorescence spectroscopy, synchronous fluorescence spectroscopy (SFS) is a valuable tool to analyze and separate the contributions in multicomponent spectra due to band narrowing, thus improving analytical selectivity. In our case, SFS was applied to solutions of **1a**, **1c**, **2a**, and **2c** after addition of CSA in order to

separate clearly the contributions from the neutral and protonated molecules. The corresponding results are shown in Figure S22 (Supporting Information) taken with an offset between the excitation and detection wavelength of 20 nm. After observation of the SFS spectra, two clear bands can be observed, one at 350–400 nm, attributed to the neutral molecules, and one at 560–620 nm due to the protonated ones. The bands are clearly well separated and better resolved than in the fluorescence spectra.

The 2D fluorescence spectra of **1a**, **1c**, **2a**, and **2c** with defined amounts of CSA are shown in Figure S23 (Supporting Information) and it is clear that for **1c** the contribution of the protonated species is small. Nevertheless, excitation of compounds **1a**, **2a**, and **2c** at 360–380 nm led to an emission that covered almost the whole visible spectrum. However, excitation at wavelengths longer than 400 nm only led to a single emission band, which is attributed to the protonated species.

2.4. Protonation study by ^{1}H NMR spectroscopy

Protonation of compound **1b** was also studied by ^{1}H NMR spectroscopy (Figure S24). The gradual addition of trifluoroacetic acid (TFA) to a $CDCl_3$ solution of **1b** resulted in a progressive downfield shift of all signals, especially those belonging to the quinazoline ring. After the addition of 40 equivalents of TFA the quinazoline signals were shifted by 0.21–0.45 ppm. As one would expect, the positions of the remaining signals were affected to a lesser extent. The spectrum remained unaltered with higher amounts of acid (up to 300 equivalents). The absence of two sets of signals for mixtures of neutral and protonated **1b** indicates a fast proton exchange in solution.

2.5. Time resolved spectroscopy in solution

The changes in the excited state dynamics of the compounds in series **1** and **2** were studied on the fs-ps and ns timescale. The dynamics were detected at the main fluorescence band of the neutral species as well as at the fluorescence band of the protonated molecules

upon increasing the amount of acid. The initial fluorescence dynamics at the main band, i.e., within the first 10 ps, are shown in Figure 7 for **1a**–**1c**, while the corresponding results for **2a**–**2c** are presented in Figure S25 (Supporting Information). In all cases, a rapid decrease of the fluorescence intensity, which mostly took place on the < 1 ps timescale, was observed when the amount of CSA exceeded a certain value, which was characteristic for each chromophore. The amplitude of this ultrafast quenching mechanism increased with the amount of acid. For example, in the case of **1a** (Figure 7a), after addition of nine equivalents of CSA the dynamics were governed by a ~ 50 fs decay followed by a 500 fs with corresponding amplitudes of 75 and 12%, respectively, thus revealing dynamic quenching of the fluorescence of the neutral molecules due to the addition of CSA. Upon addition of four equivalents of CSA, similar decay times were found but with smaller/larger amplitudes of the ultrafast/fast component of 28 and 16%, respectively. It is interesting that in **1b**, with 20 equivalents of CSA, the rapid decrease of the fluorescence intensity due to the quenching upon protonation was followed by a slight increase, which was also observed in the dynamics without acid, and this can be attributed to solvation. However, the dynamics of the protonated molecules did not change upon addition of CSA (Figure S26, Supporting Information).

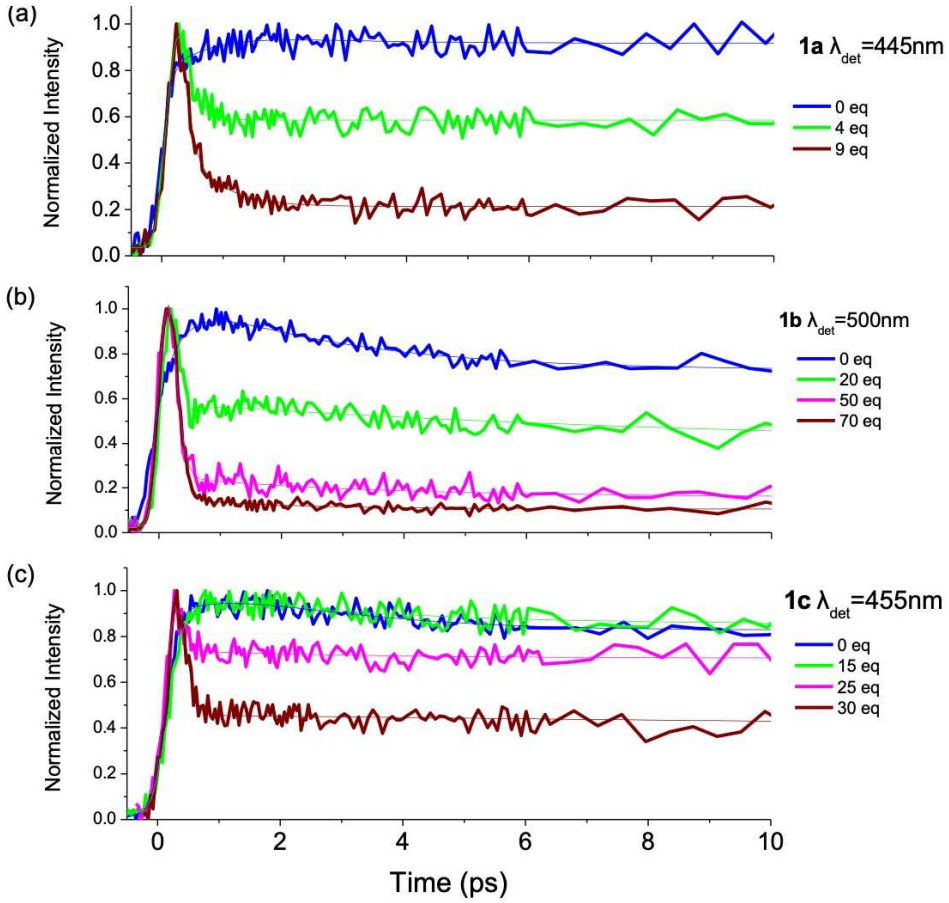

Figure 7. Fluorescence dynamics on the 10 ps timescale for (a) **1a**, (b) **1b**, and (c) **1c** upon addition of various amounts of CSA as shown in the figures. The dynamics were detected at the peak of the main fluorescence band, λ_{exc} = 385 nm.

Apart from the quenching within the first few ps, the ns fluorescence dynamics were also examined in order to observe the change in the excited state lifetime upon addition of CSA. The decays were detected at the fluorescence bands of both the neutral and protonated species. The decays for the compounds in series **1** detected at the fluorescence band of the neutral molecules are shown in Figure 8 and the corresponding results for series **2** are shown in Figure S27 (Supporting Information). In general, the decays were fitted by multi-exponential functions and the average lifetimes of the neutral chromophores decreased either slightly (**1a**, **1b**, **2b**, **2c**) or significantly (**1c**, **2a**) upon addition of acid due to the emergence of non-radiative channels and the decrease of the amplitude of the main population decay lifetime. The fitting parameters are given in Tables S3–S8 (Supporting Information). As an

example, **1c** exhibited a single-exponential decay in CH_2Cl_2 with a 3.9 ns lifetime (Figure 8c). The decays became faster upon increasing the amount of CSA, but when the amount of CSA exceeded 19 equivalents a very short mechanism (< 0.02 ns, i.e., smaller than the instrument response function of the nanosecond time-resolved system) dominated the decay. This short mechanism was better revealed in the fs-ps measurements (Figure 7). The decays regarding the emission band of the protonated species, namely at 560–620 nm, are presented in Figure S28 and the corresponding fitting parameters are summarized in Tables S9–S12 of the Supporting Information. Once again, multiexponential functions were used to fit the decays better, while the average lifetimes of the protonated molecules ranged between 1.3 and 3.5 ns and these were unaffected by increasing the amount of CSA.

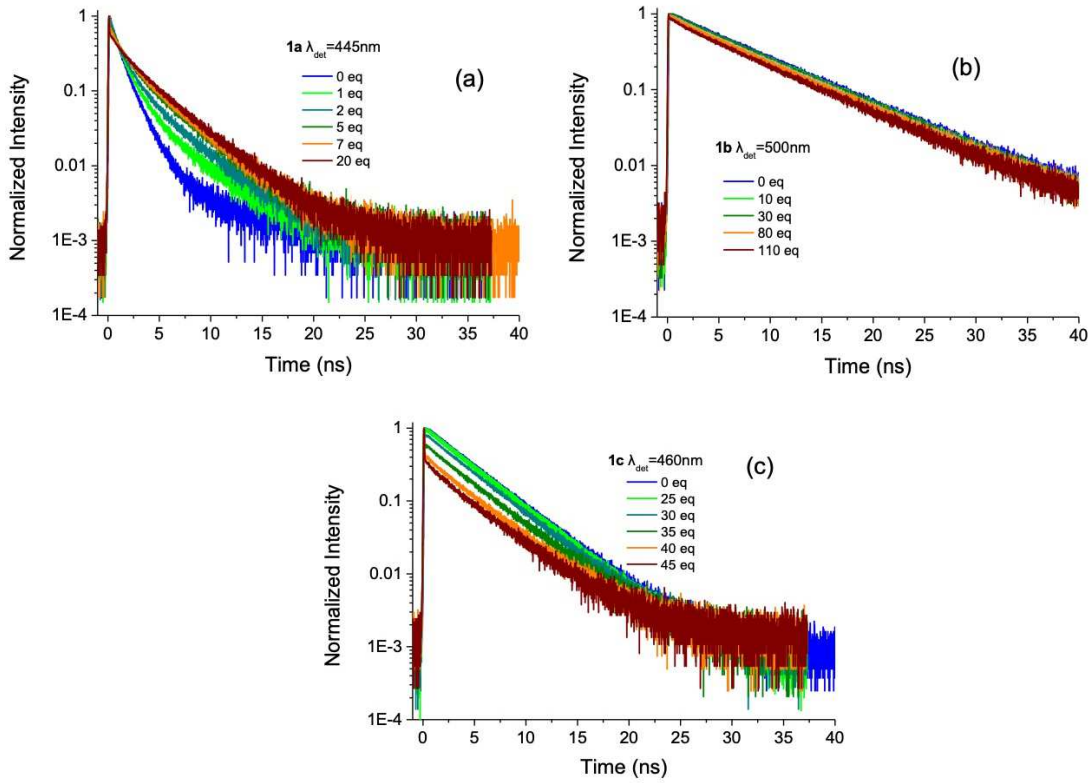

Figure 8. Fluorescence decays on the ns timescale for (a) **1a**, (b) **1b**, and (c) **1c** upon addition of various amounts of CSA as shown in the figures. The dynamics were detected at the peak of the main fluorescence band, λ_{exc} = 400 nm.

2.6. Photophysical properties in thin film

Simple thin films of polystyrene doped with 1 wt% of the quinazoline derivatives **1a, 2a**, and **2c** were prepared by spray deposition on glass substrates. Films were prepared from both neutral and fully protonated forms and these exhibited a significant blue-shifted emission with regard to their emissions in solution (Table 6), a phenomenon that was generally observed with similar azaheterocyclic push-pull derivatives.[31-33] This blue shift resulted in a mixture of two non-complementary colors and prevented the emission of white light by partial protonation of **1a** (Table 6, Figure S29 in the Supporting Information). Nevertheless, the addition of 0.85 and 0.5 equivalents of CSA to the solutions of **2a** and **2c** used for spray deposition, respectively, resulted in films that showed white photoluminescence when irradiated at 365 nm, with chromaticity coordinates close to those of pure white (Table 6, Figures 10 and S30). In order to examine better the white light emission from **2c**, the nanosecond dynamics for a film of **2c** with 0.5 equivalents of CSA (detected at both emission bands) were studied upon high-energy excitation at 400 nm (Figure 9c). The decays at 430 nm showed a rapid decrease of the intensity, while at 600 nm a slow increase was observed, which indicates an energy transfer process between neutral and protonated species. Such an energy transfer has been recognized in the past as the working mechanism in white OLEDs based on partial protonation.[35] The existence of an energy transfer is also supported by the detection of the decay at 600 nm upon lower energy excitation at 470 nm, i.e., upon selective excitation at the absorption band of the protonated species. It is clear that the increase in the dynamics, which is characteristic of the energy transfer, is absent (Figure 9c).

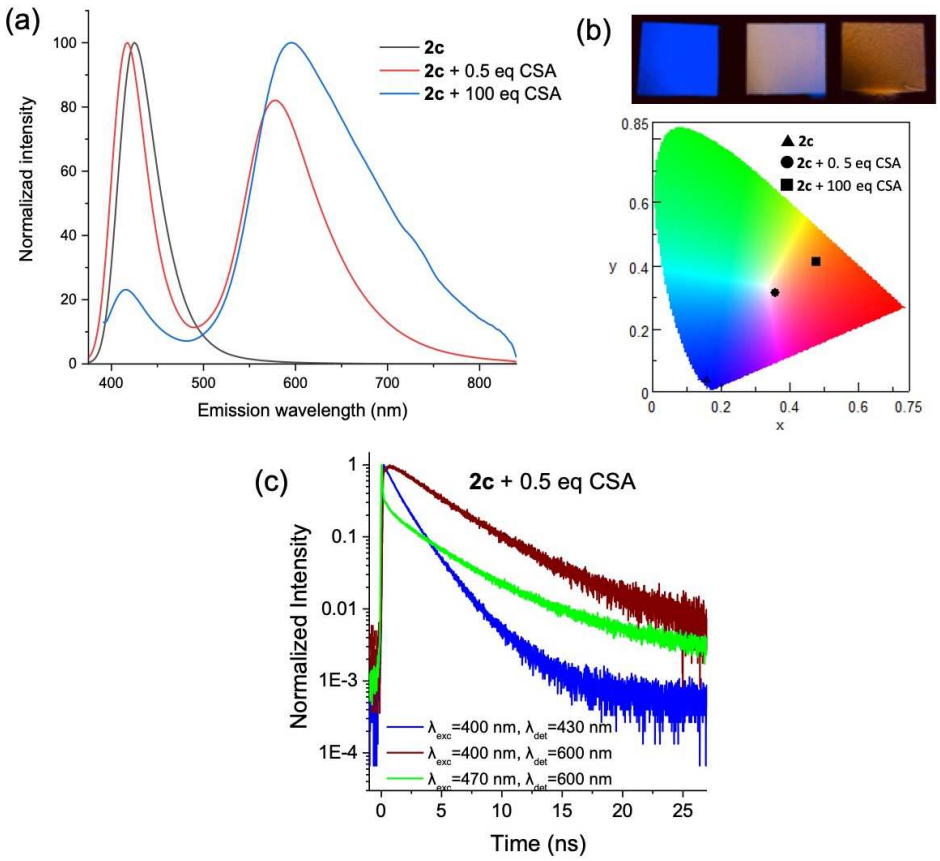

Figure 9. (a) Fluorescence spectra (λ_{exc} = 365 nm) and (b) colors of polystyrene thin films doped with **2c** (1 wt%) in the absence and the presence of 0.5 and 100 equivalents of CSA (from left to right). Photographs were taken in the dark upon irradiation with a hand-held UV lamp (λ_{exc} = 365 nm, 24 W). Also in (b) chromaticity of the fluorescence colors in a 1931 CIE diagram. (c) Fluorescence decays on the ns timescale for a film of **2c** in PS with 0.5 equivalents of CSA, detected at the two emission bands upon excitation at 400 nm and 470 nm.

Table 6. PL data and CIE coordinates of thin films of polystyrene doped with 1 wt% of quinazolines **1a**, **2a**, and **2c**.

Compd	λ_{em} (nm)		Chromaticity coordinates (x,y)[a]		
	Neutral form	Protonated form	Neutral form	Protonated form	Mixture of neutral and protonated forms
1a	419	508	(0.16, 0.08)	(0.26, 0.48)	(0.19, 0.32)[b]
2a	416	558	(0.16, 0.05)	(0.40, 0.47)	(0.26, 0.33)[c]
2c	423	595	(0.16, 0.04)	(0.48, 0.41)	(0.36, 0.31)[d]

[a] λ_{exc} = 365 nm in all cases. [b] 0.5 equivalents of CSA. [c] 0.85 equivalents of CSA. [d] 0.5 equivalents of CSA.

3. Conclusions

A new series of push-pull 4-substituted and 4,7-disubstituted quinazolines has been prepared efficiently by Suzuki–Miyaura reactions. The compounds were fully characterized using a variety of techniques. Carbazolyl and methoxynaphthyl groups were incorporated as electron-donating groups. Optical studies revealed that all of the compounds absorb light in the UV region and emit blue-green light upon irradiation, with large Stokes shifts observed. The positive emission solvatochromism confirmed the formation of an intramolecular charge-separated emitting state. The molecules can be easily protonated on the heterocyclic ring. Protonation of compounds **1b** and **2b** was accompanied by a quenching of the fluorescence, whereas compounds **1a**, **1c**, **2a**, and **2c** remained emissive and the addition of acid led to the appearance of a new red-shifted band in the fluorescence spectra. The controlled partial protonation resulted in multicolor photoluminescence, including white light, both in solution and in solid state. DFT calculations indicate that the protonation occurs preferentially on the nitrogen at position 1 even if the population of monoprotonated species at position 3 is not negligible. HOMO-LUMO energy gaps are affected very little by the addition of a second substituent but are significantly decreased by protonation. The changes in the excited state dynamics were studied by time resolved spectroscopy, with dynamic quenching of the fluorescence band of the neutral species observed upon protonation within a few tens of fs.

4. Experimental part

4.1. General information

All solvents were reagent grade for synthesis and spectroscopic grade for photophysical measurements. 4-Chloroquinazoline and 7-bromo-4-chloroquinazoline were purchased from Accela and the boronic acids were purchased from Sigma-Aldrich or TCI and were used without further purification. NMR spectra were recorded in $CDCl_3$ on a Bruker Avance Neo 500 spectrometer. The chemical shifts δ are reported in ppm and are referenced

to the residual protons of the deuterated solvent or carbon nuclei (^{1}H, δ = 7.27 ppm; ^{13}C, δ = 77.0 ppm). The coupling constants *J* are given in Hz. In the ^{1}H NMR spectra, the following abbreviations are used to describe the peak patterns: s (singlet), d (doublet), t (triplet), q (quadruplet), m (multiplet). In the ^{13}C NMR spectra, the nature of the carbons (C, CH, CH_2 or CH_3) was determined by performing a DEPT experiment. Acidic impurities in $CDCl_3$ were removed by treatment with solid K_2CO_3. Melting points (°C) were measured on a Büchi M-565 apparatus and are uncorrected. MALDI-TOF mass spectra were obtained on a Bruker Autoflex II spectrometer (no matrix was needed). High-resolution mass analyses were carried out at the 'Centre Régional de Mesures Physiques de l'Ouest' (CRMPO, Université de Rennes 1) using a Bruker MicroTOF-Q II instrument. UV-visible and fluorescence spectroscopy studies in solution were conducted on a Jasco V-750 spectrophotometer and Jasco FP-8300 or Spex Fluoromax-3 Jobin-Yvon Horiba spectrofluorimeters, respectively. All solutions were measured with optical densities below 0.1. Fluorescence quantum yields (±10%) were determined relative to the indicated reference. Thin films were prepared by the direct nebulization of CH_2Cl_2 solutions of polystyrene doped with the appropriate compound (1 wt%, in the absence and the presence of CSA) on various heated glass substrates through a fine spray nozzle powered by an air compressor system. The fluorescence spectra of these films were recorded on a Jasco FP-8300 spectrofluorimeter at λ_{exc} = 365 nm. The fluorescence dynamics on the fs-ps timescale were measured by a femtosecond time-resolved fluorescence method based on the upconversion technique.[52,53] The dynamics were measured under magic angle conditions and the samples were excited at 385 nm, which corresponds to the second harmonic of a Ti:Sapphire fs laser emitting 80 fs pulses at 770 nm. The samples were placed in a 1 mm path-length specific cell that was continuously rotated, and had an optical density below 0.1 at the excitation wavelength. The instrument response function (IRF) was ~ 250 fs. The fluorescence

decays on the ns timescale were detected by means of the Time Correlated Single Photon Counting technique using either a 400 nm or 470 nm diode laser with an 80 ps pulse duration as the excitation source. The IRF of the ns time-resolved technique was ~ 100 ps.[54]

4.2. Computational details

All calculations were performed with the Gaussian16 code.[55] Geometry optimizations for the different compounds were followed by frequency calculations to ensure the true nature of the energy minimum, at the PBE0[56] /6-311+G(d,p) level, and the solvent effects were included trough the Polarizable Continuum Model (PCM).[57] A similar protocol using the CAM-B3LYP[58] range-separated functional was also applied for additional data presented in the Supporting Information.

4.3. General procedure for Suzuki–Miyaura cross-coupling reactions

A mixture of 4-chloroquinazoline or 7-bromo-4-chloroquinazoline (1 mmol), the appropriate boronic acid (1.1 or 2.2 mmol, respectively), $Pd(AcO)_2$ (5 mol%), PPh_3 (10 mol%), aqueous Na_2CO_3 (5 mmol, dissolved in the minimum amount of water), and glyme (5 mL) was degassed by bubbling Ar through for 10 min. The reaction mixture was stirred in a pressure tube at the indicated temperature (100–140 ºC) for 22–23 h. After removing the glyme under reduced pressure, the reaction mixture was diluted with water and extracted with CH_2Cl_2 (×3). The combined organic layers were dried ($MgSO_4$), filtered through a short pad of Celite, and concentrated under vacuum. The crude product was purified by flash chromatography on neutral alumina (eluent, mixtures of hexanes/EtAcO of increasing polarity and a few drops of Et_3N) and/or washing with the indicated solvent.

4-(6-Methoxynaphthalen-2-yl)quinazoline (1a). Prepared from 4-chloroquinazoline (200 mg, 1.22 mmol), 6-methoxy-2-naphthaleneboronic acid (270 mg, 1.34 mmol), $Pd(AcO)_2$ (14 mg, 0.062 mmol), PPh_3 (32 mg, 0.122 mmol), aqueous Na_2CO_3 (646 mg, 6.1 mmol,

dissolved in the minimum amount of water), and glyme (6 mL). The mixture was heated at 100 ºC for 22 h. Purification by flash chromatography and washing with MeOH gave the title compound as a colorless solid. Yield: 190 mg (55%). Mp 135–136 ºC (EtAcO/MeOH). ^{1}H NMR ($CDCl_3$, 500 MHz): δ 3.99 (s, 3H, OCH_3), 7.25–7.27 (m, 2H), 7.64 (ddd, 1H, ^{4}J = 1.0 Hz, ^{3}J = 7.0 Hz, ^{3}J = 8.5 Hz), 7.87–7.91 (m, 2H), 7.93–7.96 (m, 2H), 8.15 (d, 1H, ^{3}J = 8.5 Hz), 8.24–8.26 (m, 2H), 9.42 (s, 1H, H2). ^{13}C NMR and DEPT ($CDCl_3$, 125 MHz): δ 168.4 (C), 158.9 (C), 154.7 (CH), 151.2 (C), 135.4 (C), 133.6 (CH), 132.3 (C), 130.3 (CH), 130.1 (CH), 128.9 (CH), 128.4 (C), 127.7 (CH), 127.5 (CH), 127.3 (CH), 123.3 (C), 119.7 (CH), 105.7 (CH), 55.4 (CH_3). MALDI-TOF MS (no matrix): *m*/*z* 287.3 $[M + H]^+$. HRMS (ESI/ASAP, TOF): *m*/*z* calculated for $C_{19}H_{15}N_2O$ $[M + H]^+$ 287.1179; found 287.1177.

4-[4-(Carbazol-9-yl)phenyl]quinazoline (1b). Prepared from 4-chloroquinazoline (200 mg, 1.22 mmol), 4-(9*H*-carbazol-9-yl)phenylboronic acid (368 mg, 1.28 mmol), $Pd(AcO)_2$ (14 mg, 0.062 mmol), PPh_3 (32 mg, 0.122 mmol), aqueous Na_2CO_3 (646 mg, 6.1 mmol, dissolved in the minimum amount of water), and glyme (6 mL). The mixture was heated at 130 ºC for 23 h. Purification by flash chromatography and washing with MeOH gave the title compound as a colorless solid. Yield: 210 mg (46%). Mp 195–197 ºC (EtAcO/MeOH). ^{1}H NMR ($CDCl_3$, 500 MHz): δ 7.35 (ddd, 2H, ^{4}J = 1.0 Hz, ^{3}J = 7.0 Hz, ^{3}J = 8.0 Hz), 7.47 (ddd, 2H, ^{4}J = 1.0 Hz, ^{3}J = 7.5 Hz, ^{3}J = 8.5 Hz), 7.58 (d, 2H, ^{3}J = 8.0 Hz), 7.73 (ddd, 1H, ^{4}J = 1.0 Hz, ^{3}J = 7.0 Hz, ^{3}J = 8.0 Hz), 7.84 (d, 2H, ^{3}J = 8.5 Hz), 8.00 (ddd, 1H, ^{4}J = 1.0 Hz, ^{3}J = 7.5 Hz, ^{3}J = 8.5 Hz), 8.08 (d, 2H, ^{3}J = 8.5 Hz), 8.19 (d, 2H, ^{3}J = 8.0 Hz), 8.20 (d, 1H, ^{3}J = 8.0 Hz), 8.31 (d, 2H, ^{3}J = 8.5 Hz), 9.46 (s, 1H, H2). ^{13}C NMR and DEPT ($CDCl_3$, 125 MHz): δ 167.4 (C), 154.7 (CH), 151.3 (C), 140.5 (C), 139.6 (C), 135.9 (C), 133.9 (CH), 131.6 (CH), 129.1 (CH), 128.0 (CH), 127.0 (CH), 126.8 (CH), 126.1 (CH), 123.7 (C), 123.1 (C), 120.4 (CH), 120.4 (CH), 109.8 (CH). MALDI-TOF MS (no matrix): *m*/*z* 372.3 $[M + H]^+$. HRMS (ESI/ASAP, TOF): *m*/*z* calculated for $C_{26}H_{18}N_3$ $[M + H]^+$ 372.1495; found 372.1499.

4-[(9-Ethylcarbazol-3-yl)]quinazoline (1c). Prepared from 4-chloroquinazoline (100 mg, 0.61 mmol), 9-ethylcarbazole-3-boronic acid (160 mg, 0.67 mmol), $Pd(AcO)_2$ (7 mg, 0.031 mmol), PPh_3 (16 mg, 0.061 mmol), aqueous Na_2CO_3 (323 mg, 3.05 mmol, dissolved in the minimum amount of water), and glyme (3 mL). The mixture was heated at 130 ºC for 22 h. Purification by flash chromatography and washing with boiling hexanes gave the title compound as a pale yellow solid. Yield: 90 mg (46%). Mp 125.5–126.5 ºC. ^{1}H NMR ($CDCl_3$, 500 MHz): δ 1.52 (t, 3H, ^3J = 7.5 Hz, CH_3), 4.48 (q, 2H, ^3J = 7.5 Hz, CH_2), 7.30 (ddd, 1H, ^4J = 1.0 Hz, ^3J = 8.0 Hz, ^3J = 9.0 Hz), 7.50 (d, 1H, ^3J = 8.5 Hz), 7.53–7.56 (m, 1H), 7.61 (d, 1H, ^3J = 8.5 Hz), 7.65 (ddd, 1H, ^4J = 1.0 Hz, ^3J = 6.5 Hz, ^3J = 8.0 Hz), 7.94 (ddd, 1H, ^4J = 1.5 Hz, ^3J = 7.0 Hz, ^3J = 8.5 Hz), 7.98 (dd, 1H, ^4J = 1.0 Hz, ^3J = 8.5 Hz), 8.15 (d, 1H, ^3J = 8.5 Hz), 8.18 (d, 1H, ^3J = 8.0 Hz), 8.34 (dd, 1H, ^4J = 0.5 Hz, ^3J = 8.5 Hz), 8.61 (dd, 1H, ^4J = 0.5 Hz, ^3J = 1.5 Hz), 9.41 (s, 1H, H2). ^{13}C NMR and DEPT ($CDCl_3$, 125 MHz): δ 169.0 (C), 154.7 (CH), 151.3 (C), 141.0 (C), 140.5 (C), 133.4 (CH), 128.8 (CH), 127.9 (CH), 127.7 (C), 127.7 (CH), 127.5 (CH), 126.3 (CH), 123.5 (C), 123.2 (C), 123.0 (C), 122.9 (CH), 120.8 (CH), 119.5 (CH), 108.9 (CH), 108.6 (CH), 37.8 (CH_2), 13.8 (CH_3). MALDI-TOF MS (no matrix): *m/z* 324.3 $[M + H]^+$. HRMS (ESI/ASAP, TOF): *m/z* calculated for $C_{22}H_{18}N_3$ $[M + H]^+$ 324.1495; found 324.1496.

4,7-Bis(6-methoxynaphthalen-2-yl)quinazoline (2a). Prepared from 7-bromo-4-chloroquinazoline (100 mg, 0.41 mmol), 6-methoxy-2-naphthaleneboronic acid (182 mg, 0.902 mmol), $Pd(AcO)_2$ (5 mg, 0.02 mmol), PPh_3 (11 mg, 0.04 mmol), aqueous Na_2CO_3 (217 mg, 2.05 mmol, dissolved in the minimum amount of water), and glyme (3 mL). The mixture was heated at 120 ºC for 22 h. Purification by flash chromatography and washing with MeOH gave the title compound as a colorless solid. Yield: 90 mg (50%). Mp 231–233 ºC ($CHCl_3$/MeOH). ^{1}H NMR ($CDCl_3$, 500 MHz): δ 3.97 (s, 3H, OCH_3), 4.00 (s, 3H, OCH_3), 7.21–7.28 (m, 2H), 7.86 (d, 1H, ^3J = 9.0 Hz), 7.89–7.98 (m, 4H), 7.93–7.96 (m, 2H), 8.02 (dd,

1H, ^{4}J = 2.0 Hz, ^{3}J = 9.0 Hz), 8.19 (s, 1H), 8.28 (s, 1H), 8.32 (d, 1H, ^{3}J = 9.0 Hz), 8.44 (d, 1H, ^{4}J = 2.0 Hz), 9.43 (s, 1H, H2). ^{13}C NMR and DEPT ($CDCl_3$, 125 MHz): δ 168.0 (C), 158.9 (C), 158.4 (C), 155.2 (CH), 151.8 (C), 146.2 (C), 135.4 (C), 134.6 (C), 134.3 (C), 132.3 (C), 130.3 (CH), 130.1 (CH), 130.0 (CH), 129.1 (C), 128.4 (C), 127.8 (CH), 127.7 (CH), 127.5 (CH), 127.3 (CH), 127.3 (CH), 126.8 (CH), 126.1 (CH), 125.6 (CH), 122.2 (C), 119.7 (CH), 119.6 (CH), 105.7 (CH), 105.6 (CH), 55.4 (CH_3), 55.4 (CH_3). MALDI-TOF MS (no matrix): *m*/*z* 443.3 $[M + H]^+$. HRMS (ESI/ASAP, TOF): *m*/*z* calculated for $C_{30}H_{23}N_2O_2$ $[M + H]^+$ 443.1754; found 443.1756.

4,7-Bis[4-(carbazol-9-yl)phenyl]quinazoline (2b). Prepared from 7-bromo-4-chloroquinazoline (100 mg, 0.41 mmol), 4-(9*H*-carbazol-9-yl)phenylboronic acid (259 mg, 0.902 mmol), $Pd(AcO)_2$ (5 mg, 0.02 mmol), PPh_3 (11 mg, 0.04 mmol), aqueous Na_2CO_3 (217 mg, 2.05 mmol, dissolved in the minimum amount of water), and glyme (3 mL). The mixture was heated at 140 ºC for 22 h. Purification by washing with a boiling mixture of EtAcO/MeOH gave the title compound as a colorless solid. Yield: 160 mg (64%). Mp 261–263 ºC (EtAcO/MeOH). ^{1}H NMR ($CDCl_3$, 500 MHz): δ 7.33–7.38 (m, 4H), 7.46–7.51 (m, 4H), 7.55 (d, 2H, ^{3}J = 8.5 Hz), 7.61 (d, 2H, ^{3}J = 8.0 Hz), 7.80 (d, 2H, ^{3}J = 8.5 Hz), 7.89 (d, 2H, ^{3}J = 8.5 Hz), 8.06 (d, 2H, ^{3}J = 8.5 Hz), 8.07 (dd, 1H, ^{4}J = 2.0 Hz, ^{3}J = 9.0 Hz), 8.15 (d, 2H, ^{3}J = 8.5 Hz), 8.20 (t, 4H, ^{3}J = 7.0 Hz), 8.45 (d, 1H, ^{3}J = 8.5 Hz), 8.51 (d, 1H, ^{4}J = 1.5 Hz), 9.51 (s, 1H, H2). ^{13}C NMR and DEPT ($CDCl_3$, 125 MHz): δ 167.2 (C), 155.4 (CH), 151.8 (C), 145.6 (C), 140.6 (C), 140.5 (C), 139.8 (C), 138.5 (C), 138.0 (C), 135.9 (C), 131.7 (CH), 129.1 (CH), 127.6 (CH), 127.4 (CH), 127.1 (CH), 126.6 (CH), 126.2 (CH), 126.1 (CH), 123.7 (C), 123.6 (C), 122.2 (C), 120.5 (CH), 120.4 (CH), 120.3 (CH), 109.8 (CH). MALDI-TOF MS (no matrix): *m*/*z* 613.5 $[M + H]^+$. HRMS (ESI/ASAP, TOF): *m*/*z* calculated for $C_{44}H_{29}N_4$ $[M + H]^+$ 613.2387; found 613.2385.

4,7-Bis[(9-ethylcarbazol-3-yl)]quinazoline (2c). Prepared from 7-bromo-4-chloroquinazoline (100 mg, 0.41 mmol), 9-ethylcarbazole-3-boronic acid (216 mg, 0.902 mmol), $Pd(AcO)_2$ (5 mg, 0.02 mmol), PPh_3 (11 mg, 0.04 mmol), aqueous Na_2CO_3 (217 mg, 2.05 mmol, dissolved in the minimum amount of water), and glyme (3 mL). The mixture was heated at 140 ºC for 23 h. Purification by flash chromatography and washing with a boiling mixture of EtAcO/MeOH gave the title compound as a pale yellow solid. Yield: 150 mg (71%). Mp 255–258 ºC (dec.) (EtAcO/MeOH). ^{1}H NMR ($CDCl_3$, 500 MHz): δ 1.51 (t, 3H, ^3J = 7.5 Hz, CH_3), 1.54 (t, 3H, ^3J = 7.5 Hz, CH_3), 4.45 (q, 2H, ^3J = 7.5 Hz, CH_2), 4.49 (q, 2H, ^3J = 7.5 Hz, CH_2), 7.29–7.33 (m, 2H), 7.47 (d, 1H, ^3J = 8.0 Hz), 7.50–7.58 (m, 4H), 7.63 (d, 1H, ^3J = 8.5 Hz), 7.95 (dd, 1H, ^4J = 2.0 Hz, ^3J = 8.5 Hz), 8.04 (dd, 1H, ^4J = 2.0 Hz, ^3J = 8.5 Hz), 8.07 (dd, 1H, ^4J = 2.0 Hz, ^3J = 8.5 Hz), 8.21 (d, 2H, ^3J = 7.5 Hz), 8.41 (d, 1H, ^3J = 8.5 Hz), 8.45 (d, 1H, ^4J = 2.0 Hz), 8.56 (d, 1H, ^4J = 2.0 Hz), 8.67 (d, 1H, ^4J = 1.0 Hz), 9.42 (s, 1H, H2). ^{13}C NMR and DEPT ($CDCl_3$, 125 MHz): δ 168.6 (C), 155.1 (CH), 151.9 (C), 147.0 (C), 141.0 (C), 140.5 (C), 140.5 (C), 140.2 (C), 130.1 (C), 128.1 (CH), 128.0 (C), 127.9 (CH), 127.4 (CH), 126.3 (CH), 126.2 (CH), 125.5 (CH), 125.4 (CH), 123.7 (C), 123.2 (C), 123.0 (C), 123.0 (C), 122.8 (CH), 122.0 (C), 120.8 (CH), 120.6 (CH), 119.6 (CH), 119.5 (CH), 119.3 (CH), 109.1 (CH), 108.8 (CH), 108.8 (CH), 108.6 (CH), 37.8 (CH_2), 37.7 (CH_2), 13.9 (2 × CH_3). MALDI-TOF MS (no matrix): *m*/*z* 517.3 $[M + H]^+$. HRMS (ESI/ASAP, TOF): *m*/*z* calculated for $C_{36}H_{29}N_4$ $[M + H]^+$ 517.2387; found 517.2387.

Acknowledgments

J. R.-L. thanks the Ministerio de Economía y Competitividad/Agencia Estatal de Investigación/FEDER for financial support (project CTQ2017-84561-P). Funding from the Junta de Comunidades de Castilla-La Mancha/FEDER is also gratefully acknowledged by J. R.-L. and S. A. (project SBPLY/17/180501/000214). DFT calculations were performed at

ISCR and the work was granted access to the HPC resources of TGCC/CINES/IDRIS under the allocation 2020-A0080800649 made by Grand Equipement National de Calcul Intensif (GENCI).

References

[1] S. Achelle, J. Rodríguez-López, F. Robin-le Guen, *ChemistrySelect* **2018**, *3*, 1852-1886

[2] G. N. Lipunova, E. V. Nosova, V. N. Charushin, O. N. Chupakhin, *Curr. Org. Synth.* **2018**, *15*, 793-814.

[3] P. Meti, H.-H. Park, Y.-D. Gong, *J. Mater. Chem. C* **2020**, *8*, 352-379.

[4] R. Komatsu, H. Sasabe, J. Kido, *J. Photon. Energy* **2018**, *8*, 032108.

[5] E. V. Nosova, S. Achelle, G. N. Lipunova, V. N. Charushin, O. N. Chupakhin, *Russ. Chem. Rev.* **2019**, *88*, 1128-1178.

[6] J. Rodríguez-Aguilar, M. Vidal, C. Pastenes, C. Aliaga, M. C. Rezende, M. Domínguez, *Photochem. Photobiol.* **2018**, *94*, 1100-1108.

[7] D. S. Kopchuk, N. V. Chepchugov, E. S. Starnovskaya, A. F. Khasanov, A. P. Krinochkin, S. Santra, G. V. Zyryanov, P. Das, A. Majee, V. L. Rusinov, V. N. Charushin, *Dyes. Pigm.* **2019**, *167*, 151-156.

[8] S. Achelle, F. Robin-le Guen, *J. Photochem. Photobiol. A : Chem.* **2017**, *348*, 281-286.

[9] K. Hoffert, R. J. Durand, S. Gauthier, F. Robin-le Guen, S. Achelle, *Eur. J. Org. Chem.* **2017**, 523-529.

[10] R. Cinar, J. Nordmann, E. Dirksen, T. J. J. Müller, *Org. Biomol. Chem.* **2013**, *11*, 2597-2604.

[11] T. N. Moshkina, E. V. Nosova, G. N. Lipunova, M. S. Valova, V. N. Charushin, *Asian J. Org. Chem.* **2018**, *7*, 1080-1084.

[12] D.-J. Park, P. Meti, Y.-D. Gong, *Dyes Pigm.* **2020**, *176*, 108254.

[13] S. Achelle, I. Nouira, B. Pfaffinger, Y. Ramondenc, N. Plé, J. Rodríguez-López, *J. Org. Chem.* **2009**, *74*, 3711-3717.

[14] H. Muraoka, N. Iwabuchi, S. Ogawa, *Bull. Chem. Soc. Jpn.* **2019**, 92, 1358-1369.

[15] V. Schmitt, S. Moschel, H. Detert, *Eur. J. Org. Chem.* **2013**, 5655-5669.

[16] C. Hadad, S. Achelle, I. López-Solera, J. C. García-Martínez, J. Rodríguez-López, *Dyes Pigm.* **2013**, *97*, 230-237.

[17] S. Achelle, J. Rodríguez-López, F. Bureš, F. Robin-le Guen, *Dyes Pigm.* **2015**, *121*, 305-311.

[18] A. Boländer, D. Kieser, C. Voss, S. Bauer, C. Schön, S. Burgold, T. Bittner, J. Hölzer, R. Heyney-von Haußen, G. Mall, V. Goetschy, C. Czech, H. Knust, R. Berger, J. Herms, I. Hilger, B. Schmidt, *J. Med. Chem.* **2012**, *55*, 9170-9180.

[19] B. Zhu, T. Zhang, Q. Jiang, Y. Li, Y. Fu, J. Dai, G. Li, Q. Qi, Y. Cheng, *Chem. Commun.* **2018**, *54*, 11558-11561.

[20] B. Dumat, G. Bordeau, A. I. Aranda, F. Mahuteau-Betzer, Y. El Harfouch, G. Metgé, F. Charra, C. Fiorini-Debuisschert, M.-P. Teulade-Fichou, *Org. Biomol. Chem.* **2012**, *10*, 6054-6061.

[21] E. V. Verbitskiy, A. A. Baranova, K. I. Lugovik, M. Z. Shafikov, K. O. Khokhlov, E. M. Cheprakova, G. L. Rusinov, O. N. Chupakhin, V. N. Charushin, *Anal. Bioanal. Chem.* **2016**, *408*, 4093-4101.

[22] E. V. Verbitskiy, A. A. Baranova, K. I. Lugovik, K. O. Khokhlov, E. M. Cheprakova, Z. Shafikov, G. L. Rusinov, O. N. Chupakhin, V. N. Charushin, *Dyes Pigm.* **2017**, *137*, 360-371.

[23] J.-P. Malval, M. Cranney, S. Achelle, H. Akdas-Kiliç, J.-L. Fillaut, N. Cabon, F. Robin-le Guen, O. Soppera, Y. Molard, *Chem. Commun.* **2019**, *55*, 14331-14334.

[24] R. Tang, X. Wang, W. Zhang, X. Zhuang, S. Bi, W. Zhang, F. Zhang, *J. Mater. Chem. C* **2016**, *4*, 7640-7648.

[25] Y. Zhan, P. Yang, G. Li, Y. Zhang, Y. Bao, *New J. Chem.* **2017**, *41*, 263-270.

[26] Z. Wu, J. Sun, Z. Zhang, P. Gong, P. Xue, R. Lu, *RSC Adv.* **2016**, *6*, 97293-97301.

[27] U. Giovanella, E. Cariati, E. Lucenti, M. Pasini, F. Galeotti, C. Botta, *ChemPhysChem* **2017**, *18*, 2157-2161.

[28] S. Achelle, J. Rodríguez-López, F. Bureš, F. Robin-le Guen, *Chem. Rec.* **2020**, *20*, 440-451.

[29] M. Li, Y. Yuan, Y. Chen, *ACS App. Mater. Interfaces* **2018**, *10*, 1237-1243.

[30] S. Achelle, J. Rodríguez-López, C. Katan, F. Robin-le Guen, *J. Phys. Chem. C* **2016**, *120*, 26986-26995.

[31] S. Achelle, J. Rodríguez-López, N. Cabon, F. Robin-le Guen, *RSC Adv.* **2015**, *5*, 107396-107399.

[32] S. Achelle, J. Rodríguez-López, M. Larbani, R. Plaza-Pedroche, F. Robin-le Guen, *Molecules* **2019**, *24*, 1742.

[33] J. Tydlitát, S. Achelle, J. Rodríguez-López, O. Pytela, T. Mikýsek, N. Cabon, F. Robin-le Guen, D. Miklík, Z. Růžičková, F. Bureš, *Dyes Pigm.* **2017**, *146*, 467-478.

[34] J. Yang, X. Liu, Z. Liu, L. Wang, J. Sun, Z. Guo, H. Xu, H. Wang, B. Zhao, G. Xie, *J. Mater. Chem. C* **2020**, *8*, 2442-2450.

[35] D. Liu, Z. Zhang, H. Zhang, Y. Wang, *Chem. Commun.* **2013**, *49*, 10001-10003.

[36] C. Hansch, A. Leo, R. W. Taft, *Chem. Rev.* **1991**, *91*, 165-195.

[37] H. C. Brown, D. H. McDaniel, O. Häfliger, in *Determination of Organic Structures by Physical Methods*, E. A. Baude, F. C. Nachod, Eds., Academic Press: New York, **1955**, pp. 567-662.

[38] E. V. Nosova, T. N. Moshkina, G. N. Lipunova, D. S. Kopchuk, P. A. Slepukhin, I. V. Baklanova, V. N. Charushin, *Eur. J. Org. Chem.* **2016**, 2876-2881.

[39] B. Li, Z. Wang, S.-J. Su, F. Guo, Y. Cao, Y. Zhang, *Adv. Opt. Mater.* **2019**, *7*, 1801496.

[40] M. J. Mphahlele, H. K. Paumo, A. M. El-Nahas, M. M. El-Hendawy, *Molecules*, **2014**, *19*, 795-818.

[41] M. J. Mphahlele, H. K. Paumo, L. Rhyman, P. Ramasami, *Molecules*, **2015**, *20*, 14656-14683.

[42] T. N. Moshkina, P. Le Poul, A. Barsella, O. Pytela, F. Bureš, F. Robin-le Guen, S. Achelle, E. V. Nosova, G. N. Lipunova, V. N. Charushin, *Eur. J. Org. Chem.*, **2020**, 5445-5454.

[43] Z. Wang, H. Li, Z. Peng, Z. Wang, Y. Wang, P. Lu, *RSC Adv.* **2020**, *10*, 30297-30303.

[44] S. Achelle, J. Rodríguez-López, F. Robin-le Guen, *J. Org. Chem.* **2014**, *76*, 7564-7571.

[45] A. B. Patel, K. H. Chikhalia, P. Kumari, *Med. Chem. Res.* **2014**, *23*, 2338-2346.

[46] Y. Kabri, P. Verhaeghe, A. Gellis, P. Vanelle, *Molecules* **2010**, *15*, 2949-2961.

[47] A. F. Littke, G. C. Fu, *Angew. Chem. Int. Ed.* **2002**, *41*, 4176-4211.

[48] S. J. P. Marlton, B. I. McKinnon, B. Ucur, J. P. Bezzina, S. J. Blanksby, A. J. Trevitt, *J. Phys. Chem. Lett.* **2020,** *11*, 4226-4231.

[49] R. Lartia, C. Allain, G. Bordeau, F. Schmidt, C. Fiorini-Debuisschert, F. Charra, M.-P. Teulade-Fichou, *J. Org. Chem.* **2008**, *73*, 1732-1744.

[50] C. Katan, M. Charlot, O. Mongin, C. Le Droumaguet, V. Jouikov, F. Terenziani, E. Badaeva, S. Tretiak, M. Blanchard-Desce, *J. Phys. Chem. B* **2010**, *114*, 3152-3169.

[51] C. Reichardt, *Chem. Rev.* **1994**, *94*, 2319-2358.

[52] F. Kournoutas, K. Seintis, N. Karakostas, J. Tydlitát, S. Achelle, G. Pistolis, F. Bureš, M. Fakis, *J. Phys. Chem. A* **2019**, *123*, 417-428.

[53] K. Seintis, D. Agathangelou, D. Cvejn, N. Almonasy, F. Bureš, V. Giannetas, M. Fakis, *Phys. Chem. Chem. Phys*. **2017**, *19*, 16485-16497.

[54] F. Kournoutas, I. K. Kalis, M. Fecková, S. Achelle, M. Fakis, *J. Photochem. Photobiol. A: Chem.* **2020***, 391*, 112398.

[55] Gaussian 16, Revision B.01, M. J. Frisch, G. W. Trucks, H. B. Schlegel, G. E. Scuseria, M. A. Robb, J. R. Cheeseman, G. Scalmani, V. Barone, G. A. Petersson, H. Nakatsuji, X. Li, M. Caricato, A. V. Marenich, J. Bloino, B. G. Janesko, R. Gomperts, B. Mennucci, H. P. Hratchian, J. V. Ortiz, A. F. Izmaylov, J. L. Sonnenberg, D. Williams-Young, F. Ding, F. Lipparini, F. Egidi, J. Goings, B. Peng, A. Petrone, T. Henderson, D. Ranasinghe, V. G. Zakrzewski, J. Gao, N. Rega, G. Zheng, W. Liang, M. Hada, M. Ehara, K. Toyota, R. Fukuda, J. Hasegawa, M. Ishida, T. Nakajima, Y. Honda, O. Kitao, H. Nakai, T. Vreven, K. Throssell, J. A. Montgomery, Jr., J. E. Peralta, F. Ogliaro, M. J. Bearpark, J. J. Heyd, E. N. Brothers, K. N. Kudin, V. N. Staroverov, T. A. Keith, R. Kobayashi, J. Normand, K. Raghavachari, A. P. Rendell, J. C. Burant, S. S. Iyengar, J. Tomasi, M. Cossi, J. M. Millam, M. Klene, C. Adamo, R. Cammi, J. W. Ochterski, R. L. Martin, K. Morokuma, O. Farkas, J. B. Foresman, D. J. Fox, Gaussian, Inc., Wallingford CT, **2016**.

[56] C. Adamo, V. Barone, *J. Chem. Phys.*, **1999**, *110*, 6158-6170.

[57] J. Tomasi, B. Mennucci, R. Cammi, *Chem. Rev.*, **2005**, *105*, 2999-3093.

[58] T. Yanai, D. P. Tew, N. C. Handy, *Chem. Phys. Lett.*, **2004**, *393*, 51-57.